Polyhedron 31 (2012) 176–187

Contents lists available at SciVerse ScienceDirect

Polyhedron

journal homepage: www.elsevier.com/locate/poly

NMR, potentiometric and ESI-MS combined studies on the zinc(II) magnesium(II) and calcium(II) complexation by (morpholin-1-yl)methane-1,1-diphosphonic acid and its thio-analog

Ewa Matczak-Jon [a,*], Barbara Kurzak [b], Wanda Sawka-Dobrowolska [c]

[a] Department of Chemistry, Wrocław University of Technology, Wybrzeże Wyspiańskiego 27, 50-370 Wrocław, Poland
[b] Faculty of Chemistry, University of Opole, Oleska 48, 45-052 Opole, Poland
[c] Faculty of Chemistry, University of Wrocław, Joliot-Curie 14, 50-383 Wrocław, Poland

ARTICLE INFO

Article history:
Received 12 July 2011
Accepted 7 September 2011
Available online 16 September 2011

Keywords:
Bisphosphonates
X-ray structures
Complex-formation equilibria
NMR
Potentiometry
ESI-MS

ABSTRACT

The crystal structures of the two derivatives of aminomethane-1,1-diphosphonic acid with morpholinyl- (**1**) and thiomorpholinyl- (**2**) side chains were determined by single crystal X-ray diffraction and discussed with respect to molecular geometry and solid state organization. The protonation equilibria, solution behavior and complex-formation equilibria in solutions of **1** and **2** with the Zn(II), Mg(II) and Ca(II) ions were studied by means of NMR, pH-potentiometry and ESI-MS methods.

As the $pK_{(NH^+)}$ protonation constants of **1** and **2** are high (11.65 and 11.91, respectively) two different approaches were used to evaluate the pH-potentiometric data. The first approach disregarded the proton-dissociation from the NH^+ group. In the second one, all the pK_a values were considered in the M(II):ligand formation equilibria. For **1**, the accuracy of the $pK_{(NH^+)}$ determination was shown to be sufficient to calculate reliable stability constants of metal complexes with the use of both approaches. For **2**, only approach neglecting the $pK_{(NH^+)}$ protonation constant was shown to be correct.

The studied acids form dinuclear, $[M_2L_3H_x]$, $[M_2L_2H_x]$ and mononuclear MLH_x and ML_2H_x complexes with different degree of ligand protonation. Tendency to undergo some oligomerization with the increase in the metal and ligand concentration was demonstrated for the [CaLH] complex of **1** and **2**. As far as **1** and **2** remain protonated, the Zn(II), Mg(II) and Ca(II) ions are coordinated exclusively through oxygen atoms of the phosphonate groups. The metal promoted proton dissociation from the NH^+ ring atom takes place in alkaline pH.

1. Introduction

Bisphosphonates (Scheme 1) are the most important class of drugs used for the treatment of diseases characterized by abnormal bone resorption such as Paget's disease, osteoporosis, skeletal complications associated with malignancy, multiple myeloma or bone metastasis arising from the breast or prostate carcinomas [1–6], thought they can also act on cells and tissues outside the skeleton. It has been demonstrated that some bisphosphonates activate human γδ T cells [7–9] and have promising antiparasitic [10–15], antibacterial [10,16] and herbicidal [17,18] properties.

As a class of compounds, bisphosphonates share a common P–C–P sequence, which is resistant to chemical and enzymatic degradation. Moreover, it enables enormous number of modifications by an attachment of the R^1 and/or R^2 side chains to the carbon atom. Commonly R^1 is OH or H atom, while the R^2 moiety is a major variable determining physicochemical, therapeutic and toxicological properties of each individual compound.

At now, bisphosphonates with one or more nitrogen atoms in the R^2 moiety (NBP's) are considered as the most potent [19–23]. Their activity is a result of two key properties. Firstly, they bind firmly to hydroxyapatite, $(Ca_{10}(PO_4)_6(OH)_2)$, which enables their accumulation at sites of bone resorption [2,19–21]. Secondly, they act intracellularly by targeting the farnesyl pyrophosphate synthase (FPPS) [24–30], which is a key enzyme in the mevalonate pathway common in human, parasite and plant cells. Both these processes require metal ions coordination through oxygen atoms of the *gem*-phosphonate groups. An exceptional affinity to bone is a result of an interaction with Ca(II) ions located on the hydroxyapatite surface. Indeed, some nitrogen-containing bisphosphonates increase their affinity to bone by the formation of N–H···O hydrogen bonds with hydroxyapatite [2]. On the other hand, an intracellular action requires bisphosphonate binding to three Mg(II) ions located in the FPPS active site. As a result, bisphosphonates impair synthesis of mevalonate metabolites and therefore osteoclasts function.

* Corresponding author. Tel.: +48 71 320 41 34; fax: +48 71 320 43 60.
E-mail address: ewa.matczak-jon@pwr.wroc.pl (E. Matczak-Jon).

0277-5387/$ - see front matter © 2011 Elsevier Ltd. All rights reserved.
doi:10.1016/j.poly.2011.09.007

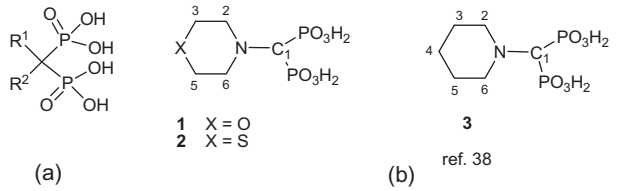

Scheme 1.

The exact nature of *in vivo* interactions between exogenous bisphosphonates and endogenous Mg(II) and Ca(II) ions is not well understood. It is postulated that bisphosphonates are endocytosed inside osteoclasts as Ca(II)-chelating microprecipitates and then released from calcium complexes upon acidification of endocytic vesicles. Metal chelates, which precipitate easily in systematic circulation are thought to be removed fast by the clearance organs [2,21]. Thus, solubility of bisphosphonate complexes with magnesium and calcium seems to be of great importance for their biological activities. On the other hand, parasitic protozoa accumulate bisphosphonates in calcium-storage organelles named acidocalcisomes, which besides calcium contain high concentration of other ions such as Mg(II), Zn(II), Na(I) or K(I) [31,32]. In this view, systematic solution studies on the complex-forming abilities of structurally diverse bisphosphonates are of great importance for understanding their structure–activity relations.

Our investigations focus predominantly on the class of compounds with a side-chain nitrogen atom attached directly to the α-carbon (Scheme 1b) [33–37]. Previously, we demonstrated complex-forming abilities of (pyridin-2-yl)aminomethane-1,1-diphosphonic acids [34], (piperid-1-yl)methane-1,1-diphosphonic acids [35] and some derivatives containing 1,3-thiazolyl, 1,3-benzothiazolyl [34], alkyl or pyrolid-1-yl [36] side chains. A vast majority of these compounds show tendency for the formation of soluble, protonated multinuclear complexes, which is especially notable at 1:1 metal to ligand ratio, in the intermediate pH range and at higher concentrations [33]. A very specific behavior was observed for a series of (pyridin-2-yl)aminomethane-1,1-diphosphonic acids, which display exceptionally slow (on the NMR time scale) complex-formation processes complicated additionally by the intramolecular *Z*/*E* interconversion [34].

Herein we report the crystal structures and complex-forming abilities of (morpholin-1-yl)methane-1,1-diphosphonic acid (**1**) and (thiomorpholin-1-yl)methane-1,1-diphosphonic acid (**2**). Both **1** and **2** may be regarded as close analogs of (piperid-1-yl)methane-1,1-diphosphonic acid (**3**), in which atom C4 is replaced by the O or S atom (Scheme 1b). Our studies are targeted at discerning similarities and differences between the Zn(II), Mg(II) and Ca(II) complexation to **1**, **2** and **3** [35,38], taking into consideration their acid–base properties, intramolecular dynamics and aggregational predispositions deduced based on crystal structures.

It was demonstrated that **1** and **2** activate γδ T cells [9] and are micromolar inhibitors of the *Leishmania major* FPP synthase [12] as well as *Plasmodium falciparum* [13] and *Toxoplasma gondi* [15] growth, being only slightly less active than **3** and its ring-substituted analogs. It is generally agreed, however, that bisphosphonates with heterocyclic side chains such as **1**–**3** are less active than bisphosphonates with heteroaromatic side chains [12,13,15,37].

2. Experimental

2.1. Materials

Compounds **1** and **2** were obtained according to the previously described procedures [39]. The metal(II) stock solutions for potentiometric measurements were prepared from MCl_2 Titrisol (Merck) concentrates. The exact metal ion concentration was checked by complexometric ethylenediaminetetraacetate (EDTA) titration. Carbonate-free potassium hydroxide solution (the titrant) was prepared from KOH and standardized against a standard potassium hydrogen phthalate solution. HCl solution was purchased from Merck as a Titrisol concentrate for preparation of stock solutions. The exact concentrations of Titrisol stock solutions and the ligand stock solutions were determined by the Gran's method [40]. All solutions were prepared with the use of bi-distilled water.

Nitrate salts of Zn(II), Mg(II) and Ca(II) (Aldrich) were used as a source of the metal ions in the NMR and ESI-MS studies.

All chemicals and solvents were used without further purification.

2.2. Methods

2.2.1. Crystal structure determination

The crystals of **1** and **2** were obtained after slow evaporation from water solutions. The crystallographic measurements were performed on a Kuma KM4CCD automated four-circle diffractometer with the graphite-monochromatized Mo Kα radiation. The data for the crystals were collected at 100(2) K using the Oxford Cryosystem cooler. The summary of the conditions for the data collection and the structure refinement parameters are given in Table 1.

The structures of both crystals were solved by direct methods using the SHELXL-97 [41] program, and refined by a full-matrix least-squared technique using SHELXS-97 [42] with anisotropic thermal parameters for non-hydrogen atoms. All H atoms in **1** and **2** were found in the difference-Fourier map and were refined isotropically. In **1**, the extinction was also refined with the final extinction amounting 0.0042(12). The data for **2** were analytically corrected for absorption with the use of CRYSALIS RED program [43].

In **2**, the H(6) atom of the phosphonic group and the H(3W) atom of the H_3O^+ ion lie on the twofold axis and on the center of inversion. The H_3O^+ cations related by the center of symmetry form the Zundel cation, $[H_2O\cdots H\cdots OH_2]^+$ [44], with both O···H distances equal to 1.220 Å and the O···O distance [2.442(2) Å] being typical for a strong hydrogen bond.

Table 1
Crystal data and structure refinement for **1** and **2**.

	1	**2**
Formula	$C_5H_{13}NO_7P_2$	$C_5H_{15}NO_7P_2S$
Formula weight	261.10	295.18
T, K	100(2)	100(2)
Crystal system	triclinic	monoclinic
Space group	$P\bar{1}$	C2/c
a (Å)	8.923(2)	14.496(3)
b (Å)	9.750(2)	8.822(2)
c (Å)	13.453(3)	19.098(4)
α (°)	108.96(3)	
β (°)	93.55(2)	97.94(3)
γ (°)	112.17(3)	
V (Å^3)	1004.3(5)	2292.3(9)
Z	4	8
Crystal size (mm)	0.30 × 0.20 × 0.020	0.30 × 0.20 × 0.08
θ Range (°)	3.68–27.50	3.38–30.0
D_{calc} (g cm^{-3})	1.727	1.711
Index ranges	$-11 \leqslant h \leqslant 10$	$-15 \leqslant h \leqslant 20$
	$-12 \leqslant k \leqslant 12$	$-12 \leqslant k \leqslant 12$
	$-17 \leqslant l \leqslant 17$	$-25 \leqslant l \leqslant 23$
μ (Mo Kα) (mm^{-1})	0.451	0.581
Absorption correction		analytical
T_{min}/T_{max}		0.840/0.950
No. of reflections collected	11 159	15 411
No. of independent reflections	4602 (R_{int} = 0.019)	3343 (R_{int} = 0.029)
Goodness-of-fit (GOF) on F^2	1.086	1.084
Final R_1, wR_2 indices [$F > 4\sigma F$)]	0.0344, 0.0768	0.0298, 0.0756
Final R_1, wR_2 indices (all data)	0.0443, 0.0803	0.0360, 0.0782
$\Delta\rho_{max,\ min}$ (e Å^{-3})	0.30/−0.27	0.277/−0.197